

# Review

## Processing of molybdenum disilicide

Y.-L. JENG, E. J. LAVERNIA

*Materials Science and Engineering, Department of Mechanical and Aerospace Engineering, University of California, Irvine, CA 92717, USA*

Inspection of the scientific literature reveals that intermetallic compounds have, in recent years, attracted considerable interest as a result of their unique elevated temperature characteristics. Among the wide range of intermetallic compounds that are actively being studied, MoSi<sub>2</sub> has been singled out as a result of its unique combination of properties, which include an excellent oxidation resistance, a high modulus of elasticity, and an elevated melting point (2030 °C). In view of this interest, the present work was undertaken with the objective of providing the reader with a comprehensive review of the mechanical and oxidation behaviour of MoSi<sub>2</sub>, paying particular attention to the synergism between processing and microstructure. Accordingly, synthesis techniques, including powder metallurgy, self-propagating high-temperature synthesis, spray processing, solid-state displacement reactions, and exothermic dispersion, are critically reviewed and discussed. In addition, recent efforts aimed at using MoSi<sub>2</sub> as a matrix material in metal–matrix composites are also critically reviewed and discussed.

### 1. Introduction

Refractory metal silicides (e.g. MoSi<sub>2</sub>, NbSi<sub>2</sub>, TaSi<sub>2</sub> and WSi<sub>2</sub>) are actively being used in a wide variety of applications, including very large scale integrated (VLSI) devices (as gate materials), interconnectors, ohmic contacts, heating elements and Schottky barriers, partly due to their excellent chemical and thermal stability and low electrical resistivity [1–5]. In recent years, molybdenum disilicide (MoSi<sub>2</sub>) has attracted considerable attention [6–13] as an elevated-temperature structural material, as a result of its unique combination of physical characteristics. These include a moderate density of 6.31 g cm<sup>-3</sup>, a high melting point of approximately 2030 °C, an excellent oxidation resistance, and a high modulus at elevated temperatures. In view of these attributes, it is not surprising that MoSi<sub>2</sub> is considered to be one of the most promising candidate materials to be used in gas turbine engines expected to operate at temperatures of up to 1600 °C.

There are two critical requirements that must be satisfied in order for a structural material to be successfully utilized in elevated-temperature applications. Firstly, the material must possess attractive combinations of mechanical properties at the intended application temperature. Secondly, the oxidation resistance of the material must be sufficiently high to prevent environmental degradation during elevated temperature exposure.

In view of these requirements, the discussion that follows is divided into two parts. Firstly, recent findings on the deformation behaviour of MoSi<sub>2</sub> are succinctly reviewed, followed by a summary on the

measurement of the elastic properties of MoSi<sub>2</sub>. Secondly, the environmental behaviour of MoSi<sub>2</sub> is discussed. Although MoSi<sub>2</sub> is inherently brittle at low temperatures, it exhibits plasticity at temperatures above the brittle–ductile transition temperature (BDTT, ~1000 °C). Accordingly, when MoSi<sub>2</sub> is deformed at temperatures below 1000 °C, fracture often occurs without significant plastic deformation [14–16]. Interestingly, however, despite this lack of plasticity, a significant amount of slip markings ( $\{110\}\langle 3\bar{3}1\rangle$ ) near the fracture surface have been observed [15–17]. Moreover, in these studies, dislocations and stacking faults were reported to be active during elevated temperature deformation [16], thus rendering the deformation to be relatively ductile in nature, in contrast to that exhibited by most ceramic materials. At temperatures above 1200 °C,  $\langle 100\rangle$ - and  $\langle 110\rangle$ -type dislocations have been reported to control the plastic deformation [15–20]. In studies on the deformation behaviour of SiC<sub>whisker</sub>-reinforced MoSi<sub>2</sub> metal–matrix composites (MMCs), it was reported that when tested at 1200 °C, no dislocation dissociation was observed in this material [17]. It was also suggested that the formation of stacking faults on  $\{110\}$  planes further improves the high-temperature ductility [16]. The formation of stacking faults in MoSi<sub>2</sub> has been closely related to the phase stability of the C11<sub>b</sub> tetragonal structure, relative to that of the C40 hexagonal structure [16].

The C11<sub>b</sub> structure is a long-range ordered crystal structure made up by stacking three bcc lattices along the *c* axis, as depicted in Fig. 1. This particular crystal structure is thought to be responsible for the aniso-

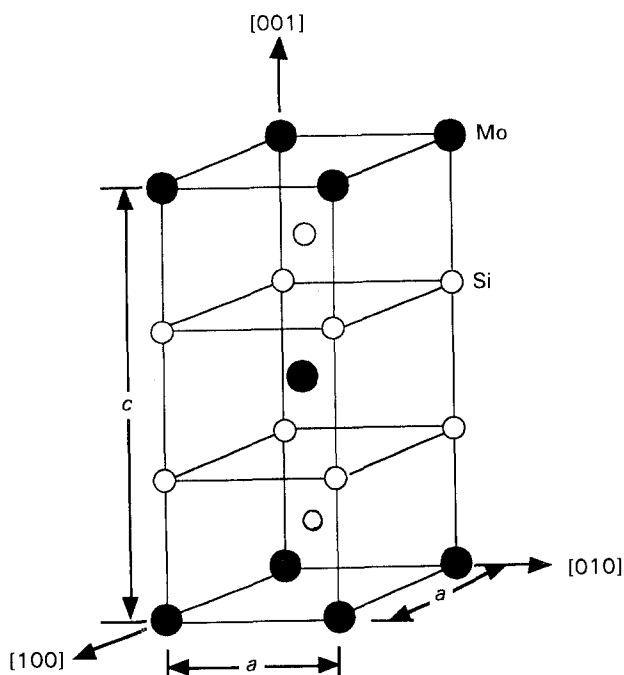


Figure 1 C11<sub>b</sub>-type tetragonal unit cell structure of MoSi<sub>2</sub>.  $a = 0.3205$ ;  $c = 0.7845$  nm [16].

trophy that is frequently associated with MoSi<sub>2</sub>. For example, compression tests on MoSi<sub>2</sub> single crystals at elevated temperatures showed that the dominant primary slip planes are the {110} planes although slip on the {013} planes was also observed [14–20]. At approximately 1900 °C, MoSi<sub>2</sub> transforms from a tetragonal (C11<sub>b</sub> type,  $a = 0.3202$ ,  $c = 0.7851$  nm) to a hexagonal (C40 type) crystal structure.

Regarding the measurement of the elastic properties of MoSi<sub>2</sub>, some information is available. Nakamura and co-workers [18], for example, used a pulse echo method involving the measurement of elastic wave velocities in different orientations of MoSi<sub>2</sub> single crystals to determine the value of the elastic constants. Moreover, on the basis of this information, and using Voigt's, Reuss's, and Hill's approximations, Nakamura and co-workers [18] determined the magnitude of the bulk modulus,  $K$ , (209.7 GPa), Young's modulus,  $E$ , (439.7 GPa), shear modulus,  $G$ , (191.1 GPa), and Poisson's ratio,  $\nu$ , (0.151) for polycrystalline MoSi<sub>2</sub>.

Regarding environmental stability, MoSi<sub>2</sub> exhibits an excellent resistance to oxidation, equivalent to that of SiC. This is evidenced by the successful utilization of MoSi<sub>2</sub> as heating elements capable of operating in air, at temperatures in excess of 1500 °C [21–25]. In particular, the best grade of MoSi<sub>2</sub> heating element, commercially known as “Kanthal Super”, is capable of operating up to a temperature of 1800 °C. This material consists of a mixture of fine MoSi<sub>2</sub> particles bonded together with an aluminosilicate ( $x\text{Al}_2\text{O}_3 \cdot y\text{SiO}_2$ ) glass phase [25]. The excellent oxidation resistance of MoSi<sub>2</sub> is attributed in part to the formation of a self-healing, glassy silica (SiO<sub>2</sub>) layer, which prevents the MoSi<sub>2</sub> matrix from undergoing further oxidation. However, this low melting-point, glassy phase is detrimental to the elevated temperature strength. The formation of weak second phase or liquid phase

along grain boundaries drastically enhances grain boundary sliding and mass transport during elevated temperature exposure, and thus reduces creep resistance. In addition, the relative low elevated temperature strength of MoSi<sub>2</sub> further diminishes the creep resistance.

On the basis of the above findings, it is evident that despite its attractive combinations of elastic properties and oxidation resistance, MoSi<sub>2</sub> is inherently brittle when deformed at temperatures below 1000 °C, and furthermore exhibits a poor creep resistance at temperatures above 1200–1300 °C. Therefore, investigators have sought to achieve further improvements in low-temperature ductility and elevated temperature strength by blending MoSi<sub>2</sub> with a soft metallic phase (e.g. ductile phase reinforcement) and a hard ceramic phase (metal matrix composites), respectively [6–13, 26–53]. Despite encouraging preliminary results obtained with these two approaches, there are various issues that must be addressed before MoSi<sub>2</sub> may be successfully utilized as an elevated temperature structural material. In MMCs, for example, thermodynamic incompatibility between the MoSi<sub>2</sub> matrix and the ceramic reinforcements may ultimately degrade the oxidation resistance of MoSi<sub>2</sub>. To that effect, the thermodynamic stability of MoSi<sub>2</sub> reinforced with various types of ceramic reinforcements has been studied extensively [9, 11, 30, 37, 40, 41, 43, 54–62] and will be discussed in a later section.

The objective of the present paper is to examine the various synthesis approaches that have been utilized in an attempt to improve the physical and mechanical behaviour of MoSi<sub>2</sub> and MoSi<sub>2</sub>-based composites. Recent research results are emphasized, paying particular attention to key fundamental issues derived from novel synthesis approaches. We begin with a discussion of processing techniques, followed by recent findings on oxidation behaviour and mechanical properties. The paper concludes with a section on creep behaviour.

## 2. Processing techniques

A wide variety of processing techniques have been successfully utilized to synthesize MoSi<sub>2</sub> and the associated composites. In the following sections, these are critically discussed, paying particular attention to recent research findings. To discuss the results in a coherent manner, the present section has been subdivided into five subsections: powder metallurgy (PM) techniques, self-propagating high temperature synthesis (SPS), spray processing, solid-state displacement reactions, and exothermic dispersion (XD<sup>TM</sup>) techniques.

### 2.1. Powder metallurgy techniques

Powder metallurgy techniques typically involve the consolidation of discrete powders into a bulk form using temperature and/or pressure. Accordingly, the present discussion is divided into three sub-sections entitled: pressure-assisted sintering, reaction sintering, and mechanical alloying.

### 2.1.1. Pressure-assisted processing techniques

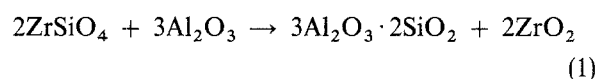
The pressure-assisted processing technique, including hot pressing, sinter forging, hot isostatic pressing (HIP), and hot extrusion, is an operation in which powder preforms are consolidated by applying pressure at elevated temperatures [63, 64]. A specific variation of this synthesis methodology, known as pressureless sintering, involves heating the powder preform in the absence of an external superimposed pressure. When applied to high-melting-point, high-strength materials, however, pressureless sintering is often time- and energy-intensive, and furthermore, often does not result in a fully dense product [63, 64]. In pressure-assisted processing, with the presence of a superimposed pressure, mechanisms such as grain rotation, grain boundary sliding, fragmentation, plastic deformation, and enhanced diffusion along grain boundaries all play a critical role in providing an enhanced densification rate which leads to reduced energy consumption, and often full densification [65–67]. Among the various pressure-assisted processing techniques, hot pressing and hot extrusion techniques typically involve heating the  $\text{MoSi}_2$  powders in a die held under uniaxial pressure to densify or deform the material to a predetermined condition. In the case of sinter forging, the procedure is similar to that of hot pressing, but no lateral constraint is required. These three techniques, hot extrusion, hot pressing and sinter forging, are relatively easy and inexpensive to operate, but unfortunately they are severely limited in terms of their ability to produce complex shapes. Hot isostatic pressing, although more elaborate and costly to operate, provides advantages, such as no density variations, almost unlimited aspect ratio, uniform grain structure and the ability of achieving very complicated shape products, over the other three techniques [63, 64]. The modelling of pressure-assisted techniques has been aggressively pursued for several decades. Unfortunately, factors such as the variations in powder packing, varying particle morphologies, the influence of friction on deformation, and environmental effects have hindered the successful development of accurate models that may ultimately be applied to real processing situations [66–69].

Among the various pressure-assisted processing techniques that are available, hot pressing is most widely used. It has been successfully utilized to process monolithic  $\text{MoSi}_2$  [7] and a wide variety of  $\text{MoSi}_2$ -based composites, such as those containing Nb- [31], W- [31], C- [32],  $\text{ZrO}_2$ - [43, 45],  $\text{Al}_2\text{O}_3$ - [46], SiC- [7, 34, 42], and TiC- [37] reinforced  $\text{MoSi}_2$ , with significant improvements in both flexure strength and fracture toughness. However, materials prepared by uniaxially hot-pressing a mixture of reinforcement and  $\text{MoSi}_2$  powders are inherently simple in shape, and due to their poor machinability, often cannot be further processed into desired shapes. It is also evident, however, that further work is needed before pressure-assisted processing techniques may be commercially used to synthesize complex shapes of  $\text{MoSi}_2$  and  $\text{MoSi}_2$ -based composites.

### 2.1.2. Reaction sintering

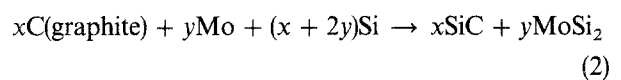
Reaction sintering processing techniques generally involve the *in situ* reaction of constituent powders, generally pressed into a preform, to produce a bulk composite preform that is different from the initial reactants [70]. Reactions can be either very fast (even explosive) or very sluggish, and either exothermic or endothermic, depending on starting and final reactant compositions, reactant compact microstructures; processing environments, and thermal boundary conditions [70]. In the discussion that follows, reaction sintering is defined as ‘reaction-assisted sintering’, which is diffusion-controlled and non-ignitable, and therefore is relatively sluggish. The high reaction rate processing techniques will be discussed in the SPS section.

Inspection of the available literature reveals that a wide variety of chemical reactions are generally involved in the preparation of structural materials using reaction techniques, ranging from powder synthesis (e.g., sol–gel technique, polymer pyrolysis, and decomposition of salts and organometallics) to direct production of a bulk material (e.g., chemical vapour deposition (CVD) and chemical vapour infiltration (CVI) techniques) [71]. However, as stated by Rice [70], although various reactions are capable of producing composite materials, of relevance are “reactions that can produce composite powders for consolidation into composites, or more commonly reactions involving a powder compact to form a composite product with the aid of heat, possibly with pressure as well, such as hot pressing, or hot isostatic pressing”. One well-known example, dating back to early 1980s, of the reaction synthesis approach involves the preparation of zirconia-toughened mullite ( $\text{ZrO}_2 + 3\text{Al}_2\text{O}_3 \cdot 2\text{SiO}_2$ ) by employing the following reaction [72]:



to form mullite–zirconia composites, which exhibited outstanding combination of mechanical properties.

Recently, Messner and Chiang [73–75] have successfully fabricated liquid-phase reaction-bonded SiC– $\text{MoSi}_2$  composites by using alloyed Si–Mo melts on the basis of the following reaction:



In this SiC– $\text{MoSi}_2$  composite,  $\text{MoSi}_2$  is utilized as a reinforcement to toughen the SiC matrix. It is worth noting that the final SiC– $\text{MoSi}_2$  composite did not contain residual Si, whose presence is highly deleterious in elevated temperature applications. The liquid-phase reaction-bonding technique not only preserves the advantages of CVI, but also significantly reduces the time required for processing, and is capable of achieving a final density of 90%. However, it has been found [73] that below the melting of  $\text{MoSi}_2$ , mixtures of Mo and Si do not react completely, and a reaction layer develops, which inhibits further reaction.

On the basis of the previous findings [73, 74], Weiser *et al.* [76] employed pressureless reaction

sintering to fabricate  $\text{MoSi}_2$ -based composites. In their work,  $\text{MoSi}_2$  matrices with either 0 or 20 vol % SiC particulate were mixed with 10 vol % of elemental Mo and Si (an atomic ratio of 1:2), and then sintered in Ar at various temperatures. The addition of elemental Mo and Si was found to greatly enhance the densification of monolithic  $\text{MoSi}_2$  at temperatures as low as  $1400^\circ\text{C}$ . However, almost no densification was found in the composites containing SiC particulates, and this result was attributed to swelling and poor consolidation resulting from the undesirable reaction between SiC and Mo–Si elemental additives.

On the basis of the above-mentioned findings, and despite encouraging preliminary results, it is evident that the optimization of process parameters during reaction sintering requires further attention. However, even if the properties that are achieved with reaction sintered materials were only comparable with those of materials processed by conventional means, reaction sintering should potentially be the preferred approach in terms of production costs. Furthermore, it may be beneficial to use pressure-assisted processing techniques, combined with reaction sintering and liquid-phase sintering, e.g. Mo–Si reaction to form  $\text{MoSi}_2$  and melting of Si, because this approach should provide a synergistic effect, not only to diminish the production costs, but also to improve mechanical behaviour.

### 2.1.3. Mechanical alloying

In recent years, the mechanical alloying (MA) technique, an application of mechano-chemistry, has attracted considerable interest [77–99]. MA involves repeated welding, fracturing and rewelding of powders (elemental or alloyed) during high-energy milling under a controlled atmosphere, as shown in Fig. 2 [77]. This process can be divided into four stages [96]:

- (i) first stage: an intense cold welding period;
- (ii) intermediate stage: a rapid fracturing period, forming lamellae;
- (iii) final stage: a moderate cold welding period, producing finer and more convoluted lamellae;
- (iv) completion stage: a steady state period.

Factors such as the amount of cold work, inter-layer spacing, and interstitial contamination critically influence the formation of compounds during MA [77]. During the high-energy milling process, repeated particle impact at contact points leads to a local concentration of energy, which under some circumstances may ignite a self-propagating reaction. This phenomenon, originally described by Atzmon [79–81] as “hot-spotting”, may lead to local melting and welding, enhanced inter-particle diffusion, chemical reaction, and ultimately to compound formation.

The mechanical alloying technique has been extensively utilized to produce a wide variety of compounds with highly refined microstructures [77–88]. Moreover, MA materials have been reported to exhibit non-equilibrium microstructural characteristics, such as the extension of solid solubilities [89, 90]. Not surprisingly, MA has been successfully used to combine alloying elements that would otherwise be unattainable by conventional techniques. One notable ex-

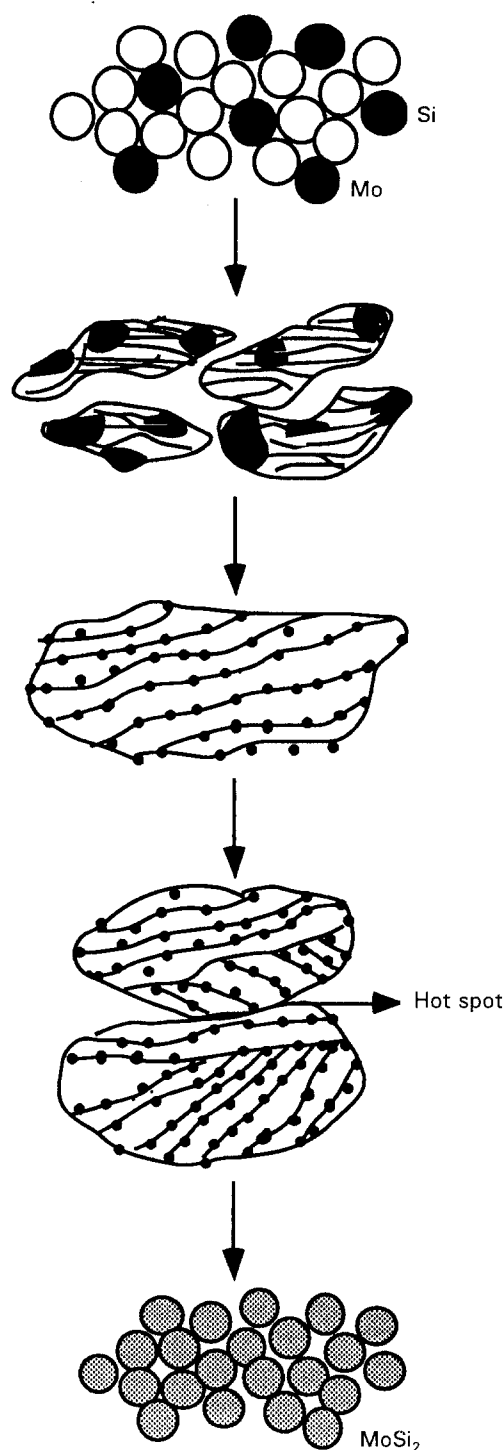


Figure 2 Schematic of  $\text{MoSi}_2$  compound formation by mechanical alloying [77].

ample is superconducting intermetallic  $\text{Nb}_3\text{Sn}$ , which is difficult to prepare by conventional melting process, due to the significant melting point difference between Nb and Sn ( $\sim 2240^\circ\text{C}$ ) [91]. The large degree of microstructural refinement that is associated with MA materials often leads to dramatic improvements in mechanical behaviour. In 1966, for example, Seybolt [92] reported a 400% improvement in the rupture strength of MA  $\text{Al}_2\text{O}_3$ –FeAl relative to that of the matrix alloy.

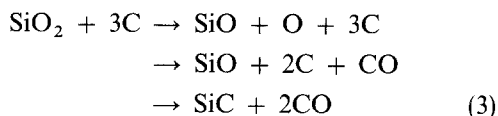
Some current applications of the MA include the production of oxide-dispersion strengthened alloys and intermetallic compounds [93, 94]; the development of oxidation and hot-corrosion resistant

coatings [95]; the alloying of otherwise immiscible systems (e.g. Cu–Pb) [96]; the production of super-corroding and superconducting (Nb–Sn) materials [91]; and the preparation of amorphous compounds [78].

Recently, MA has been applied to the fabrication of silicides [77, 78, 86, 97, 98]. Accordingly, group V transition metal/Si silicides and amorphous Ti–Si alloy powders have been produced by mechanical alloying of elemental powders [78]. In group V transition metal/silicon systems, amorphization was reported in the Ta–Si system, but not in the Nb–Si system [96]. Factors such as the highly exothermic release of heat of mixing, fast interdiffusion rates, local melting, and the presence of a high defect concentration, have all been proposed to influence amorphization, although the precise mechanisms remain to be established [82].

The formation of MoSi<sub>2</sub> was first reported by Iwatomo & Uesaka [97], during MA of elemental Mo (5 μm) and Si (50 μm) powders. In this study, it was reported that α-MoSi<sub>2</sub>, a low-temperature tetragonal phase, forms initially followed by the formation of a high-temperature hexagonal phase, normally present at temperatures in excess of 1900 °C. Following MA, the crystalline MoSi<sub>2</sub> particles were highly refined, exhibiting a grain size ranging from 5 to 10 nm. Moreover, Iwatomo & Uesaka [97] also confirmed the presence of amorphous regions in the MA MoSi<sub>2</sub> powder during prolonged milling time. The sintered MA MoSi<sub>2</sub> powders did not exhibit any significant differences in hardness or electrical conductivity when compared to equivalent material prepared using other techniques. However, the ultra-fine structure of the mechanically alloyed powders significantly reduced the sintering temperature (by nearly 400 °C), while yielding a final density in excess of 97% of theoretical [97]. Moreover, Ma *et al.* [98] reported that the formation of MoSi<sub>2</sub> by room-temperature high-energy ball milling of elemental powders is self-propagating.

Very recently, Jayashankar & Kaufman [99] used MA to synthesize *in-situ* SiC-reinforced MoSi<sub>2</sub> composites. In this work, Mo and Si powders, combined to yield the desired stoichiometry, were mixed with 4 wt % of C, followed by high-energy mechanical attrition. The overall reaction:



was proposed to describe the formation of SiC, and the simultaneous elimination of SiO<sub>2</sub> during hot pressing of mechanically alloyed MoSi<sub>2</sub> composite powders. The presence of C was found to significantly improve the overall homogeneity and cleanliness of the microstructure. Moreover, the significant weight loss noted in samples containing C was attributed to the formation of CO during MA, consistent with the results of Maloy *et al.* [32].

Schwarz *et al.* [100] recently reported a number of advantages that are available by using MA for the

synthesis of MoSi<sub>2</sub>-based alloys starting from elemental constituents: (i) higher hot-pressed density; (ii) lower hot-pressing temperatures for consolidation; (iii) better chemical homogeneity; (iv) improved room temperature hardness with second-phase additions. It is worth noting, however, that the formation of amorphous SiO<sub>2</sub> phase still occurred, although extreme care was taken during MA. In applications requiring creep resistance, it is imperative to produce MoSi<sub>2</sub> composites that are free of SiO<sub>2</sub>. Hence, in principle, the MA technique may be successfully utilized to process MoSi<sub>2</sub> and MoSi<sub>2</sub> composites, as long as careful control of impurity content and environmental control are duly exercised.

## 2.2. Self-propagating high-temperature synthesis

Chemical reactions that are accompanied by the release of thermal energy are generally referred to as exothermic reactions. Self-propagating (or self-sustaining) high-temperature synthesis, so-called SPS (or SHS), is a technique involving the propagation of a high-temperature zone, driven by a highly exothermic reaction, through a compact of reactants. Although some of the reactions that were discussed are exothermic in nature, and hence in principle should be able to self-propagate, SPS generally proceeds at reaction rates that are substantially faster relative to those present during reaction sintering. The extent of reaction,  $\eta$ , is related to the temperature profile that is present during SPS, and may be represented by the following expression [101–103]:

$$\eta(x) = \frac{C_p \rho v (T - T_0) - \kappa_1 \frac{\partial T}{\partial x}}{(\kappa_2 - \kappa_1) \frac{\partial T}{\partial x} + q \rho v} \quad (4)$$

where  $C_p$  and  $\rho$  are the heat capacity and density of the product, respectively;  $v$  the velocity of combustion wave;  $T$  the reaction temperature;  $T_0$  the initial temperature;  $\kappa_1$  and  $\kappa_2$  are the thermal conductivity of reactants and products, respectively;  $q$  is the heat of reaction; and  $x$  is the coordinate along which the combustion wave propagates.

Inspection of the available literature shows that SPS and other related techniques have been successfully used to produce a variety of alloys and composites [70, 104–118]. Early studies on transition-metal silicides prepared by SPS techniques showed that the reaction product contains one or more intermediate phases [104, 105]. In related work, Trambukis & Munir [106], and Bhattacharya [107] demonstrated that it is possible to use SPS to synthesize Ti<sub>5</sub>Si<sub>3</sub> possessing attractive elevated temperature characteristics (e.g. strength and oxidation resistance) that are suitable for engineering applications. It has been found [106] that both heating rates and particle sizes critically influence the synthesis of silicides. In this study, SPS involved two reactions: a solid-state diffusion reaction for conditions of small particle size and low heating rates, and a liquid-state reaction for large particles and high heating rates. The time period

during which diffusion was rate-controlling increased with decreasing heating rate and decreasing particle size, a trend that was also noted to result in the formation of more intermediate phases. Regarding mechanical behaviour, Bhattacharya [107] recently measured a fracture toughness of approximate  $5 \text{ MPa m}^{1/2}$  for SPS-processed 15 wt % SiC-Ti<sub>5</sub>Si<sub>3</sub> composite, and noted that the presence of SiC not only dramatically enhances fracture toughness, but also alters the kinetics and thermodynamics during SPS.

Regarding the synthesis of MoSi<sub>2</sub> by SPS, very limited studies have been conducted [106–108]. In a recent study, Deevi [108] successfully synthesized single-phase MoSi<sub>2</sub> by SPS, which involves exothermic diffusional reaction of solid Mo with liquid Si. It was found that product formation depends on the temperature and available diffusion reaction time. At low heating rates, Mo<sub>5</sub>Si<sub>3</sub> is the predominant phase prior to the melting of Si, while the amount of MoSi<sub>2</sub> phase increases with increasing heating rate. No mechanical properties and microstructural details were provided in this study.

In general, however, SPS processes typically involve relatively violent reaction rates, and thus it is often challenging to achieve a high degree of microstructural control. Inspection of the recent scientific literature, however, immediately reveals that this synthesis approach is receiving considerable attention [103, 113–118]. Some of the challenges that must be addressed if SPS processes are to live up to their potential include an accurate assessment of the relevant process economics; the minimization of residual porosity in SPS processed materials; and the development of control strategies in order to obtain reproducible microstructures and properties [103, 113–118].

### 2.3. Plasma-spray processing

Spray processes offer a unique opportunity to combine the benefits associated with fine particulate technology (e.g. microstructure refinement, alloy modifications, etc.) with *in situ* processing, and in some cases, near-net shape manufacturing. Spray-based technology has evolved over the past few decades, and as a result a variety of spray-based methods are currently available. These include low-pressure plasma deposition [28, 29], modified gas welding techniques [119], high-velocity oxyfuel thermal spraying [120] and spray atomization and deposition processing [121–126]. Spray processing generally involves highly non-equilibrium conditions, and as a result these processes offer the opportunity of modifying the properties of existing alloy systems, and developing novel alloy compositions. In principle, such an approach will inherently avoid the extreme thermal excursions, with concomitant microsegregation, that are normally associated with casting processes. Furthermore, this approach also eliminates the need to handle fine reactive particulates, normally associated with powder metallurgical processes.

Plasma technology has been researched extensively over the past four decades, and is similar to spray

deposition in that it involves the deposition of discrete droplets onto a substrate or shaped container. Unlike spray deposition, however, in which the maximum attainable temperature is of the order of 1000–3000 °C, plasma torches are capable of achieving temperatures in excess of 10<sup>4</sup> K. Accordingly, plasmas may be utilized to raise reactant temperatures high enough to make the chemical potential of the desired reaction negative, and to ensure high reaction rates.

The plasma deposition technique has been successfully utilized in a large number of commercial applications, such as in corrosion, wear enhancement and surface treatment [28, 29, 127–138]. More recently, plasma-sprayed superconductors [134] and biomedical devices [135] are actively being pursued. A plasma spraying technique, known as low vacuum plasma deposition (LVPD), has also been successfully applied to fabricate highly dense bulk composite materials. A schematic diagram showing plasma deposition is shown in Fig. 3. Under a low-vacuum environment (especially with low oxygen content), highly dense composite materials may be readily synthesized. Similar to the gas-atomization and deposition process, the LVPD technique has advantages such as very small grain size, chemical homogeneity, non-equilibrium solubility and near final-shape production. In the LVPD process, an inert gas stream, such as Ar or Ni, is commonly used to accelerate the powder particles as they are being injected into the plasma gases. Due to the high speed of the plasma gases, exceeding Mach III in some cases, the time spent from injection to deposition is almost infinitesimal (of the order of milliseconds). To obtain optimal microstructural characteristics during plasma spraying, it is therefore critical to select appropriate gun-to-substrate distances by taking into account factors such as alloy composition and particle size. If the particles are too large, for example, they will not melt completely, whereas if the particles are too small they may be vaporized by the plasma. Similarly, particle morphology has been shown to influence the final microstructure of plasma-sprayed materials and spherical particles are preferred over irregularly-shaped particles, due to the better fluidity from spherical particles which can provide a better powder feeding control and thus a better control on the final microstructure.

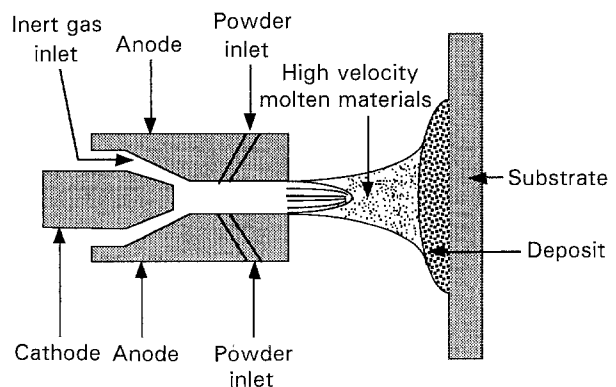


Figure 3 Schematic of plasma spray deposition processing [127].

Plasma processes may be readily utilized to prepare composite materials, simply by spraying either preblended composite particles or by simultaneously co-spraying metal and ceramic particles. In related work, Castro *et al.* [28, 29] successfully fabricated monolithic and composite MoSi<sub>2</sub> using the LVPD technique. The density of both reinforced and monolithic plasma-sprayed MoSi<sub>2</sub> was noted to be in the 95–98% range, and the materials exhibited a highly-refined microstructure. Moreover, the hardness and fracture toughness of the LVPD-processed materials were noted to be significantly improved relative to conventionally processed materials. An interesting, although not surprising, characteristic observed in the LVPD-processed material was the presence of a laminar, plate-like microstructure. When fracture tested in a direction parallel to the principal axis of the plates, preferential crack growth occurred along the prior splat-boundaries, suggesting less-than-optimum interparticle bonding. In related work, Tiwari *et al.* [132, 136] used the vacuum plasma spraying (VPS) technique to prepare monolithic, TiB<sub>2</sub>-based and SiC-based MoSi<sub>2</sub> composites. In this study, highly-dense monolithic and composite MoSi<sub>2</sub> were fabricated, with concomitant improvement in toughness response. Various reinforcement morphologies were reported, including splat-like TiB<sub>2</sub> and relatively equiaxed SiC. These morphologies were attributed to the concurrent melting of TiB<sub>2</sub> and the sublimation of SiC, respectively. It is worth noting that the oxygen content, which resulted in the formation of amorphous SiO<sub>2</sub>, was significantly increased using this technique. More recently, Jeng *et al.* [137, 138] used a plasma synthesis approach to manufacture SiC-reinforced MoSi<sub>2</sub> composites. Their work was conducted under a low vacuum environment in an industrial-scale plasma spray unit. In this study, dense composites with improved toughness were obtained. No preferential crack growth along the transverse direction (the direction perpendicular to the spray direction) was observed, indicating a well-bonded interface.

In the same study, a very high creep rate was found, and it was attributed to the formation of SiO<sub>2</sub>. The room temperature mechanical properties of plasma-sprayed MoSi<sub>2</sub>, as reported throughout the scientific literature, are summarized in Table I.

On the basis of the work reviewed in this section, it is evident that the ultra-high temperatures that are associated with commonly-utilized plasma techniques, such as LVPD, may be successfully used in the manufacture of a variety of structural materials and composites. It is also evident, however, that a fundamental understanding of the large number of interrelated variables that govern plasma processing must be achieved for this synthesis approach to live up to its enormous commercial potential.

#### 2.4. Solid-state displacement reactions

Solid-state displacement reactions may simply be described as diffusional phase transformations, involving the reaction of two or three elements or compounds to form thermodynamically stable new compounds. Early research work on this topic may be traced back to the 1930s with the pioneering work of Wagner [139–141] on the kinetics of solid-state displacement reactions of layered and aggregated materials. Several decades later, Rapp and his colleagues [142–145] extended the phenomenological treatment and theory originally proposed by Wagner [139–141] to successfully predict the arrangement of product phases during diffusional phase transformations. On the basis of these studies, Rapp *et al.* [142–146] proposed that displacement reactions between metastable oxides and reactive elements lead to the formation of two morphologies, layered or aggregated arrangements, and that the latter arrangement can be further categorized as lamellar or interwoven. The formation of different reaction product morphologies depends on the thermodynamic and kinetic parameters of the reaction system and the solubilities between the reactants and products [142, 143, 146]. When the solubilities are

TABLE I Room-temperature mechanical properties of plasma-sprayed MoSi<sub>2</sub> and MoSi<sub>2</sub>-based composites

Material condition	Hardness (VHN)	Fracture toughness (MPa m <sup>1/2</sup> )	Flexure strength (MPa)	Reference
MoSi <sub>2</sub> , HP	–	2.6	–	[43]
MoSi <sub>2</sub> , Plasma spray	1052 ± 67	5.7 ± 0.2* 2.7 ± 0.1 <sup>†</sup>	–	[28]
MoSi <sub>2</sub> , Plasma spray	1201 ± 45	4.7	280	[136]
MoSi <sub>2</sub> , Plasma spray + HIP <sup>‡</sup>	1027 ± 16	3.6 ± 0.2* 3.2 ± 0.2 <sup>†</sup>	–	[28]
MoSi <sub>2</sub> , Plasma spray + anneal <sup>§</sup>	1093 ± 25	5.9	–	[136]
20 vol % Ta + MoSi <sub>2</sub> , Plasma spray	883 ± 28	6.9 ± 0.2	–	[28]
20 vol % Ta + MoSi <sub>2</sub> , Plasma spray + HIP <sup>‡</sup>	802 ± 13	5.9 ± 0.2	–	[28]
20 vol % TiB <sub>2</sub> + MoSi <sub>2</sub> , Plasma spray	1057 ± 27	6.1	380	[136]
8.7 vol % SiC + MoSi <sub>2</sub> , Plasma spray	1158 ± 72*	4.6*	–	[137]
	1140 ± 82 <sup>†</sup>	4.2 <sup>†</sup>		

\* Spray direction (SD, longitudinal direction).

<sup>†</sup> Perpendicular to spray direction (PSD, transverse direction).

<sup>‡</sup> 206 MPa, 1200 °C for 1 h.

<sup>§</sup> 1100 °C for 24 h.

high, the reaction system tends to form an interwoven arrangement. On the other hand, if the solubilities are negligible, the layered or lamellar-arrangement morphology becomes dominant [142, 143, 146].

Inspection of the available literature shows that solid-state displacement reactions have been successfully utilized to fabricate ceramic and intermetallic matrix composites. Henager *et al.* [147, 148], for example, synthesized *in situ* MoSi<sub>2</sub>-SiC composites by using a solid-state displacement reaction between Mo<sub>2</sub>C and Si:



In this study, diffusion couples were heated in a vacuum furnace for 16 h at 1200 °C or 20 h at 1350 °C, at pressures lower than 10<sup>-4</sup> Pa. The area fraction of SiC used was determined to be about 30% and the morphology of the SiC phase was platelet-like. It was observed that prolonged exposure times at elevated temperatures led to spheroidization of the SiC particles. Moreover, microhardness indentation tests revealed that the propagation of cracks in the MoSi<sub>2</sub>-SiC did not follow a classical brittle behaviour, exhibiting crack deflection and crack wake-bridging. Unfortunately, a detailed analysis of the relevant displacement reactions was precluded by the lack of availability of the pertinent kinetic and thermodynamic data.

It is evident that solid-state reactions may be successfully used to synthesize composites and other structural materials with attractive combinations of microstructure and properties [147, 148]. Unfortunately, diffusion-controlled displacement reactions are generally sluggish and energy intensive. Therefore, from a practical standpoint, solid-state displacement reactions will be most useful when utilized in conjunction with another processing methodology, such as plasma processing or hot pressing.

### 2.5. Exothermic dispersion (XD) technique

The exothermic dispersion process, commercially designated as the XD technique, was originally developed in the Martin-Marietta Laboratories for the manufacture of composite materials containing finely dispersed ceramic or intermetallic particles, in metallic or intermetallic matrices [149-155]. As described [149, 150], in this process, elemental powders of a high temperature phase, *X* and *Y* (e.g. Ti + B) are heated in the presence of a third metallic phase, *Z* (e.g. Al), which is typically the matrix alloy. The matrix metal, *Z*, acts as a solvent and usually melts at some temperature that is well below that required to form the stable ceramic phase, *XY* (e.g. TiB<sub>2</sub>). The component elements *X* and *Y* then react exothermically, and form micrometre-sized *XY* particles in the solvent matrix. Because the dispersoids are formed during *in situ* reactions, it is possible to produce clean matrix/reinforcement interfaces that are free from extraneous contaminants. Moreover, it is possible to obtain very large amounts (> 40 vol %) of relatively well-dispersed particles, with concomitant improvements

in strength, elastic modulus and thermal stability [149, 150].

When used in combination with conventional thermomechanical techniques (e.g. rolling and extrusion), the XD<sup>TM</sup> technique may be readily used to manufacture a wide variety of metal and intermetallic matrix composites [151-154]. For example, recently the XD<sup>TM</sup> technique has been successfully used to produce composite materials that are based on the MoSi<sub>2</sub> matrix [52, 58, 155, 156]. Among the various types of reinforcement that were used in this particular investigation, TiB<sub>2</sub>, ZrB<sub>2</sub>, HfB<sub>2</sub> and SiC, the SiC-containing composites were noted to exhibit the best oxidation resistance [58, 155, 156]. The oxide that formed in SiC-reinforced MoSi<sub>2</sub> XD<sup>TM</sup> composites was noted to be a continuous layer of SiO<sub>2</sub>. Regarding low-temperature oxidation behaviour, the MoSi<sub>2</sub>-based XD<sup>TM</sup> composites did not exhibit pesting after 48 h exposure at 450, 500 or 550 °C. Moreover, the improvement in mechanical properties was found to be dependent on particle size, particle distribution, and volume fraction of the reinforcements. Finally, the MoSi<sub>2</sub>-based XD<sup>TM</sup> composites exhibited Hall-Petch strengthening at elevated temperatures, suggestive of the dislocation pile-up in the matrix-reinforcement interface region [156].

Although preliminary results obtained with this approach are encouraging, there are a few issues that need to be addressed before this approach becomes more widely utilized. For example, since the XD<sup>TM</sup> technique may be loosely classified as a controlled temperature casting, it faces similar drawbacks, such as the presence of micro- and macro-porosity, and elemental micro- and macro-segregation.

### 3. Oxidation resistance

In view of the intended utilization of MoSi<sub>2</sub> as an elevated temperature structural material, the oxidation behaviour of MoSi<sub>2</sub> and MoSi<sub>2</sub>-based composites has received considerable attention. Monolithic MoSi<sub>2</sub>, for example, when exposed to an oxidizing environment at a temperature of 500 °C, completely disintegrates into a powder-like product, a phenomenon that is generally known as "pest". Pest has been determined to be the result of preferential oxygen attack in the interparticle interface in porous MoSi<sub>2</sub> [6, 61, 62]. At temperatures below 500 °C, the protective SiO<sub>2</sub> layer has not yet been formed, and therefore weak interfaces such as grain boundaries, pores, and microcracks are readily attacked by oxygen, resulting in "pest" [61]. At temperatures between 500 and 550 °C, a transition from a low-temperature non-protective oxidation to a high-temperature protective oxidation (forming SiO<sub>2</sub>) occurs [61]. At even higher temperatures, the presence of SiO<sub>2</sub> layer prevents MoSi<sub>2</sub> from undergoing further oxidation. It has been demonstrated that the "pest" phenomenon is not generally present in fully dense MoSi<sub>2</sub>, as a result of the low bulk diffusivity of oxygen. Chou & Nieh [61, 62] studied pest phenomena and found reaction products consisting of SiO<sub>2</sub> clusters, MoO<sub>3</sub> whiskers, and residual MoSi<sub>2</sub> in both single- and poly-crystalline MoSi<sub>2</sub>. Pest reactions on single-crystalline MoSi<sub>2</sub>



TABLE II Thermodynamic compatibility between reinforcements and MoSi<sub>2</sub> and the effect of reinforcements on the oxidation resistance of MoSi<sub>2</sub>-based composites

Material	MP (°C)	Thermodynamic compatibility with MoSi <sub>2</sub>	Oxidation resistance	Reference
Nb	2468	Not compatible, formation of (Mo, Nb) <sub>5</sub> Si <sub>3</sub>	Degrading	[30]
Ta	2996	Not compatible, formation of (Mo, Ta) <sub>5</sub> Si <sub>3</sub>	Degrading	[30]
B <sub>4</sub> C	2350	Not compatible, formation of MoB <sub>2</sub> + SiC	Degrading	[40]
SiC	2300–2500	Compatible	No effect	[58]
TiC	3050–3230	Compatible	No effect	[39]
TiB <sub>2</sub>	2900	Compatible	Forming borosilicate	[60]
ZrB <sub>2</sub>	3255	Not compatible, interdiffusion of B, Si, Zr	Degrading	[58]
Si <sub>3</sub> N <sub>4</sub>	1750–1900	Compatible	No effect	[38]
Al <sub>2</sub> O <sub>3</sub>	2050	Not compatible, formation of Mo <sub>5</sub> Si <sub>3</sub> + SiO	Forming aluminosilicate	[11]
Y <sub>2</sub> O <sub>3</sub>	1750–1900	Not compatible, formation of Mo <sub>5</sub> Si <sub>3</sub> + SiO	Degrading	[41]
ZrO <sub>2</sub>	2500–2600	Not compatible, formation of ZrSiO <sub>4</sub>	Degrading	[43]
Mullite	1850	Not compatible, production of MoO <sub>3</sub>	Degrading	[57]

were limited, and only occurred on selective sites. They also found the existence of a long incubation time for pest to begin, indicating that a nucleation period, not a growth period, is the rate-limiting step for MoSi<sub>2</sub> pest.

It has been reported [157] that the oxidation behaviour of MoSi<sub>2</sub> is a function of processing conditions. HIPed or single-crystal materials, which contain no microcracking, undergo accelerated oxidation but do not fragment, while cast materials, which contain microcracks, undergo accelerated oxidation and fragmentation. In related work, Chou & Nieh [61, 62] noted that SiO<sub>2</sub> and MoO<sub>3</sub> are formed during accelerated oxidation. For oxidation temperatures between 600 and 1000 °C, internal silica formation along grain boundaries was found in the cast material, but not in the HIPed material, and this internal silica layer was often cracked. At temperatures above 1000 °C, only external silica was found in both materials. Hence, at present the best way to avoid pesting in monolithic MoSi<sub>2</sub> is to eliminate potential defects, such as microcracks and porosity, during fabrication.

As there are various types of reinforcing phases that potentially may be used to improve the low temperature toughness and selected temperature strength of MoSi<sub>2</sub> composites, it is important to examine their influence on the oxidation resistance of the composites. The thermodynamic compatibility and oxidation behaviour of MoSi<sub>2</sub>, containing various types of reinforcements, are summarized in Table II. It is worth noting that no element that may be used as a ductile phase reinforcement has yet been reported to be completely compatible with MoSi<sub>2</sub> [9, 11, 30, 31, 59]. Niobium and tantalum, for example, the two most widely investigated ductile reinforcements, react with MoSi<sub>2</sub> to form (Mo, Nb)<sub>5</sub>Si<sub>3</sub> and (Mo, Ta)<sub>5</sub>Si<sub>3</sub> compounds. Only the oxidation behaviour of Nb particulate-reinforced MoSi<sub>2</sub> has been investigated in detail [30, 31, 59]. The oxidation resistance of MoSi<sub>2</sub> was found to be severely degraded by the addition of Nb, both at high and low temperatures, due to the rapid oxidation of Nb. Therefore it is likely that the addition of other ductile reinforcement materials will have similar effects on degrading the oxidation resistance of MoSi<sub>2</sub>.

Regarding elevated temperature strength, the res-

ults summarized in Table II show that oxide reinforcements are generally not desirable, as these tend to react with the MoSi<sub>2</sub> matrix at elevated temperatures [11, 41, 43]. Despite these drawbacks, there are some oxide reinforcements that may be used in MoSi<sub>2</sub>, depending on the operating environment. Partially stabilized zirconia (PSZ), for example, is chemically compatible with MoSi<sub>2</sub> up to a temperature of 1700 °C and therefore is widely used to enhance the toughness of MoSi<sub>2</sub> [31, 43, 45, 53]. Among various borides and carbide phases that are available, SiC is often used as reinforcement in MoSi<sub>2</sub>, as it exhibits excellent oxidation resistance and it is thermodynamically stable with MoSi<sub>2</sub>. In related studies, Petrovic & Honnell [38] reported that MoSi<sub>2</sub>-reinforced Si<sub>3</sub>N<sub>4</sub> exhibited excellent combinations of mechanical properties and chemical stability up to a temperature of 1500 °C.

The results reviewed in this section reveal that the successful utilization of MoSi<sub>2</sub> composites in elevated-temperature applications requires a detailed assessment of the synergistic effects derived from factors such as chemical compatibility, oxidation resistance and mechanical behaviour. For example, although TiC [37] and MoSi<sub>2</sub> are thermodynamically compatible, the resulting composite fails to exhibit attractive combinations of mechanical properties. In the following section a discussion on the mechanical behaviour of MoSi<sub>2</sub> and MoSi<sub>2</sub> composites is presented.

#### 4. Mechanical properties

Numerous investigators have sought to improve the poor room-temperature fracture toughness and low elevated-temperature yield strength that are typically associated with MoSi<sub>2</sub>, by utilizing a variety of reinforcing phases and processing approaches. A description of the available experimental data, as summarized in Table III, reveals some encouraging results. For example, MoSi<sub>2</sub>-based composites, reinforced by 20 vol % SiC fibres, yielded a significant fracture toughness improvement from 2.5 to 8.2 MPa m<sup>1/2</sup> [35]. It was also found that 2 wt % C added to the MoSi<sub>2</sub> matrix significantly improved the elevated-temperature toughness to 11.5 MPa m<sup>1/2</sup> at 1400 °C [32].

TABLE III Mechanical properties of MoSi<sub>2</sub>-based composites by various processing conditions

Composition	Processing condition	Flexure strength (MPa)	Hardness (VHN)	Fracture toughness (MPa m <sup>1/2</sup> )	Reference
Monolithic MoSi <sub>2</sub>	Hot press	~ 250	8–10 GPa	2.5–3	[7]
10 vol % Nb + MoSi <sub>2</sub>	Hot press, 1700 °C, 30 MPa 40 min	–	–	5	[31]
10 vol % W + MoSi <sub>2</sub>	Hot press, 1700 °C, 30 MPa 40 min	–	–	~ 3	[31]
20 vol % Ta + MoSi <sub>2</sub>	LPPD	–	883 ± 28.1	6.9(SD), 4.4(PSD)	[28]
20 vol % Ta + MoSi <sub>2</sub>	LPPD + HIP	–	802 ± 12.5	5.9(SD), 4.9(PSD)	[28]
2 wt % C + MoSi <sub>2</sub>	Hot press, 1830 °C, in air	–	12.74 GPa	5.5(800 °C), 11.5(1400 °C)	[32]
25 vol % Al <sub>2</sub> O <sub>3</sub> + MoSi <sub>2</sub>	Vacuum hot press, 1500–1600 °C, 46 MPa	550 (at 1100 °C)	–	4.8(RT) 6.5(1100 °C)	[46]
20 vol % ZrO <sub>2</sub> + MoSi <sub>2</sub>	Hot press, 1700 °C, 32 MPa	–	–	7.80	[45]
30 vol % PSZ + MoSi <sub>2</sub>	Hot press, 1700 °C, 30 MPa	–	8.49 GPa	6.56	[43]
20 vol % VLS SiC + MoSi <sub>2</sub>	Hot press, 1625–1640 °C, 41.4 MPa, in CO–CO <sub>2</sub> air	310	–	8.20	[7]
20 vol % VS SiC + MoSi <sub>2</sub>	Hot press, 1800–1900 °C, in Ar	~ 280	–	6.59	[34]
20 vol % SiC + MoSi <sub>2</sub>	Hot press, 1700 °C, 35 MPa, in an inert atmosphere	263	–	6.37	[42]
30 vol % SiC + MoSi <sub>2</sub>	Displacement reaction, at 1350 °C, at 10 <sup>-4</sup> MPa	–	12.8 GPa	–	[147]
30 vol % SiC + MoSi <sub>2</sub>	Hot press & solid state reaction, at 1350 and 1700 °C	–	14.2 GPa	8.70	[147]
20 vol % SiC + 50/50 mol % MoSi <sub>2</sub> /WSi <sub>2</sub>	Hot press, 1900 °C, 30 MPa, in Ar	80 (at 1500 °C)	–	–	[27]
20 vol % TiC + MoSi <sub>2</sub>	Hot press, 1700 °C, 35 MPa, in an inert atmosphere	125.3	–	5.00	[37]
20 vol % TiB <sub>2</sub> + MoSi <sub>2</sub>	Plasma spray	380	1057 ± 27	6.10	[136]

In general, ductile reinforcements may be efficiently used to improve the low-temperature fracture toughness of MoSi<sub>2</sub> [158]. Unfortunately, as discussed in the preceding section, the ductile materials that are typically used tend to undergo extensive oxidation and chemical reactions at elevated temperatures. One approach that has been successfully utilized to minimize the reactivity experienced by these materials at elevated temperatures is to coat the ductile reinforcement. Lu *et al.* [9], for example, successfully inhibited diffusion of Si by coating the ductile phase reinforcement, in this case Nb, with Y<sub>2</sub>O<sub>3</sub>.

Similarly, Maloy *et al.* [32, 159] showed that C additions significantly improved the fracture toughness of MoSi<sub>2</sub> by avoiding the formation of SiO<sub>2</sub>. Unfortunately, extensive alloy weight loss occurred during processing, a phenomenon that was attributed to the oxidation of Mo (forming MoO<sub>3</sub>) and free Si (forming SiO). Maloy *et al.* [159] suggested that this phenomenon could be avoided by deoxidizing the MoSi<sub>2</sub> chemically prior to hot pressing and then adding SiC to the deoxidized powder.

Recent studies have shown that it is possible significantly to improve the fracture toughness of MoSi<sub>2</sub> on the basis of a ZrO<sub>2</sub> transformation toughening mechanism [31, 43, 45, 53]. The effect of ZrO<sub>2</sub> toughening is known to be closely related to the volume fraction that is present, and the extent of stabilization of ZrO<sub>2</sub>, i.e. partially stabilized ZrO<sub>2</sub>,

provides a better toughening effect than fully stabilized ZrO<sub>2</sub> [53]. For example, the room temperature fracture toughness, deduced from indentation measurements, was reportedly improved from 2.58 MPa m<sup>1/2</sup> in pure MoSi<sub>2</sub> to 6.56 MPa m<sup>1/2</sup> in 30 vol % PSZ–MoSi<sub>2</sub> [43] and 7.8 MPa m<sup>1/2</sup> in 20 vol % ZrO<sub>2</sub>–MoSi<sub>2</sub> [45]. Interestingly, the contribution of the transformation toughening mechanism to the overall toughness has been reported to be relatively small, due to the presence of other mechanisms such as grain bridging and crack branching [53]. Unfortunately, preliminary results observed by Petrovic & Honnell [43] suggested that the formation of a glassy phase during elevated temperature exposure adversely affects the mechanical properties of PSZ–MoSi<sub>2</sub>. Further work is continuing in this area to confirm the validity of this suggestion.

TiC, despite its high strength, elastic modulus and chemical inertness, does not appear to yield significant improvements in the mechanical properties of MoSi<sub>2</sub>, as evidenced by the data shown in Table III. The TiC–MoSi<sub>2</sub> interfacial bond strength appears to be high, as evidenced by the absence of crack deflection or interfacial debonding [37]. Hence the fracture behaviour of TiC-reinforced MoSi<sub>2</sub> is reportedly brittle, exhibiting a transgranular fracture morphology.

Regarding strengthening behaviour, Petrovic & Honnell [27] reported excellent elevated temperature yield strength values in a hot-pressed 20 vol % SiC-

reinforced 50/50 vol % MoSi<sub>2</sub>-WSi<sub>2</sub> composite. For example, at 1500 °C the two-phase WSi<sub>2</sub>-MoSi<sub>2</sub> matrix composites provided yield strength values which were 8–10 times higher than those of MoSi<sub>2</sub> matrix composites, and at 1200 °C the VS SiC<sub>whisker</sub>-reinforced WSi<sub>2</sub>-MoSi<sub>2</sub> matrix composites exhibited a very high yield strength of 600 MPa. The elevated temperature strength and low-temperature plasticity of MoSi<sub>2</sub> may be simultaneously improved through the addition of a homogeneous dispersion of fine phases.

The presence of an amorphous SiO<sub>2</sub> phase is generally unavoidable in MoSi<sub>2</sub>, as a result of the thermodynamic stability of this phase [160]. Interestingly, the presence of amorphous SiO<sub>2</sub> enhances sintering kinetics in MoSi<sub>2</sub> by acting as a grain boundary lubricant [161]. It is important, however, to completely eliminate SiO<sub>2</sub> upon completion of processing, because (as previously discussed) it adversely influences mechanical behaviour. To that effect additions of SiC and C have been demonstrated to eliminate SiO<sub>2</sub> [7, 12, 32]. Not surprisingly, SiC is often used to reinforce MoSi<sub>2</sub>, as a result of its synergistic effect on mechanical behaviour, oxidation resistance and thermal stability. Interestingly, the addition of SiC also appears to inhibit grain growth in SiC by inhibiting the interdiffusion between MoSi<sub>2</sub> particles [6, 7, 36]. The relative importance of the various toughness mechanisms that are active in SiC-reinforced MoSi<sub>2</sub> have been shown to depend on several factors, including SiC volume fraction and morphology [7, 36]. In SiC<sub>whisker</sub>-reinforced MoSi<sub>2</sub>, for example, crack deflection has been proposed to play a critical role in the toughening behaviour.

Monolithic MoSi<sub>2</sub> is known to be ductile at temperatures above 1000 °C, as evidenced by the presence of significant dislocation plasticity. In order to strengthen MoSi<sub>2</sub>-based composites, the volume fraction and morphology of SiC become extremely important to inhibit dislocation movement. In related studies, Battacharya & Petrovic [44] reported that an optimum level of toughness may be achieved for a SiC volume fraction of about 20%. It was suggested that further increase in the SiC volume fraction beyond this level leads to a decrease in fracture toughness, possibly due to the formation of a continuous path for crack

propagation. SiC reinforcements in fibre, whisker, or particulate forms are all capable of providing excellent mechanical property improvements. Moreover, to optimize the dispersion strengthening effect, and taking into account a volume fraction limit of 20%, it is reasonable to utilize highly refined SiC, e.g. finer particulate and smaller-diameter whiskers.

## 5. Creep behaviour

For elevated-temperature structural materials, an adequate creep resistance is one of the most important requirements. The creep behaviour of monolithic MoSi<sub>2</sub> and various MoSi<sub>2</sub>-based composites fabricated by different processing routes has been extensively studied [47–50, 137, 138, 162–166]. Some results are summarized in Table IV. Inspection of the creep rates [49, 50] and stress exponents, *n*, that have been reported by various investigators, reveal that the results are often inconsistent. A stress exponent of unity suggests that creep is controlled by diffusional mechanism, a viscous flow process. Stress exponents between 1 and 3, however, are indicative of a combination of viscous flow and dislocation motion. Finally, stress exponents greater than 3 fall into the power law creep region, typically *n* = 3 for dislocation glide and *n* = 4.5 for dislocation climb.

For a <210>-oriented single crystal MoSi<sub>2</sub>, Bose [163] reported an activation energy, *Q<sub>c</sub>*, of 251 kJ mol<sup>-1</sup> and a stress exponent of 3. A stress exponent of 3 [163] was also reported for dense polycrystalline monolithic MoSi<sub>2</sub>, indicating that creep deformation is controlled by dislocation glide. On the basis of TEM microstructural observations, Suzuki *et al.* [165, 166] found that the rate-controlling mechanism changed from dislocation glide to dislocation climb as temperature increased, corresponding to a change in activation energy. In a related study [162], the stress exponent was also found to increase with increasing strain rate and decreasing temperature in monolithic MoSi<sub>2</sub>.

Furthermore, a stress exponent of 1.75 was reported in HPed monolithic MoSi<sub>2</sub> [49, 50], suggesting the presence of the viscous SiO<sub>2</sub> along grain boundaries. Other investigators [47, 137, 162] also found low

TABLE IV Comparison of creep parameters for various monolithic MoSi<sub>2</sub> and MoSi<sub>2</sub>-based composites

Material	Test type	Temperature (°C)	Stress exponent, <i>n</i>	<i>Q<sub>c</sub></i> (KJ mol <sup>-1</sup> )	Reference
Single-crystal MoSi <sub>2</sub>	Compression	1200	3	251	[163]
MoSi <sub>2</sub> , HP (or HIP)	Compression	1200	3	306	[163]
MoSi <sub>2</sub> , HP (or HIP)	Tension	1200	3	348	[163]
MoSi <sub>2</sub> , HP	Compression	1100–1300	1.8	380	[49]
MoSi <sub>2</sub> , HP + HIP	Compression	1050–1300	3.5	430	[166]
50/50 MoSi <sub>2</sub> -WSi <sub>2</sub> , HP	Compression	1100–1400	2.3	540	[49]
9 vol % SiC + MoSi <sub>2</sub> , plasma spray	Compression	1100–1300	2.5	300	[138]
9 vol % SiC + MoSi <sub>2</sub> , plasma spray	Compression	1300–1500	1.5	190	[138]
20 vol % SiC + MoSi <sub>2</sub> , HP	Compression	1100–1400	2.6	460	[49]
30 vol % SiC + MoSi <sub>2</sub> XD™, HP + HIP	Compression	1050–1300	3	–	[166]
20 vol % SiC + MoSi <sub>2</sub> -WSi <sub>2</sub> , HP	Compression	1100	3.1	–	[47]
20 vol % SiC + MoSi <sub>2</sub> -WSi <sub>2</sub> , HP	Compression	1200	2.3	312	[164]
20 vol % SiC + MoSi <sub>2</sub> -WSi <sub>2</sub> , HP	Tension	1100–1200	3.2	557	[164]

stress exponent values, such as 1.5 [138] and 2.3 [164] in MoSi<sub>2</sub>-based composites [137, 138], indicating that the creep deformation was related to grain-boundary sliding. These results are not surprising, as the presence of a weak low-melting-point SiO<sub>2</sub> coating along grain boundaries drastically changes the controlling mechanism from a dislocation-controlled ( $n \geq 3$ ) deformation process to a viscous flow process. For example, in the LVPD-processed MoSi<sub>2</sub>-based composites [137, 138] the low vacuum processing environment results in the formation of SiO<sub>2</sub>, which not only drastically degraded the creep resistance but also negated the reinforcing effect provided by the SiC additions.

The creep behaviour of HPed or HIPed SiC-reinforced MoSi<sub>2</sub> has been studied in detail [47–50, 163–166]. Under identical testing conditions, monolithic MoSi<sub>2</sub> deformed at a much faster rate than that of the composite and showed extensive ductility, suggesting that with the additional SiC reinforcement, the creep resistance was improved. The stress exponent was in the vicinity of 3, indicating that the deformation was controlled by dislocation glide mechanisms. In related studies on monolithic MoSi<sub>2</sub>, Sadananda *et al.* [48] reported that creep deformation at elevated temperatures and high stress levels was controlled by a dislocation glide–climb mechanism, which is similar to the finding that the stress exponent increases with increasing temperature [165, 166]. Moreover, a very high stress exponent was reported in both monolithic MoSi<sub>2</sub> and MoSi<sub>2</sub>-based composites [48, 137, 138, 162] in the low stress condition, possibly due to the presence of a threshold stress or back stress.

In related work conducted by Basu & Ghosh [162], it was also suggested that both dislocation and diffusion mechanisms critically influence creep deformation in MoSi<sub>2</sub> composites reinforced with CaO, SiO<sub>2</sub> and Mo<sub>5</sub>Si<sub>3</sub> [162]. In tensile creep tests, the stress exponent and activation energy were found to be similar to that observed in compression tests [163]. However, in 20 vol % SiC-reinforced 50/50 MoSi<sub>2</sub>–WSi<sub>2</sub>, significant differences in both stress exponent and activation energy were found, with  $n = 2.3$  and  $Q_c = 312 \text{ kJ mol}^{-1}$  in compression against  $n = 3.2$  and  $Q_c = 557 \text{ kJ mol}^{-1}$  in tension.

Based on the above findings, the observed high stress exponent values can be attributed to a threshold stress phenomenon at the low stress condition and a change in rate controlling mechanism from dislocation glide to dislocation climb as temperature increases. The SiO<sub>2</sub> phase should be completely eliminated for improved creep resistance. As discussed above, the stress exponent is generally in the vicinity of 3 in both monolithic and composite MoSi<sub>2</sub>, suggesting that dislocation motion is responsible for the creep deformation.

## 6. Summary

The excellent elevated-temperature characteristics of MoSi<sub>2</sub> have been well established for several decades, as evidenced by the widespread utilization of these materials as heating elements. The body of literature

reviewed in the present paper reveals that improvement in two critical areas must be accomplished before MoSi<sub>2</sub> may be successfully utilized as a structural material. These are in the low-temperature toughness and elevated temperature strength behaviour of MoSi<sub>2</sub>. Despite the encouraging results that have been achieved by incorporating various materials in MoSi<sub>2</sub>, composite-based MoSi<sub>2</sub> introduces a tertiary challenge, namely optimizing the chemical compatibility and oxidation behaviour of MoSi<sub>2</sub> composites. On the basis of the available scientific data, it appears that among various types of reinforcements, SiC additions to MoSi<sub>2</sub> lead to attractive combinations of strength, oxidation resistance and thermal stability. Unfortunately, the room-temperature toughness of SiC/MoSi<sub>2</sub> composites is improved (over that of unreinforced MoSi<sub>2</sub>) only after a toughening mechanism such as ductile phase toughening is incorporated in the material. Moreover, the fundamental information that is necessary to determine optimal combinations of factors such as reinforcement size, volume fraction and geometry, are essentially non-existent.

Regarding synthesis techniques, the present paper reveals that there are a wide variety of routes readily available to prepare MoSi<sub>2</sub> and MoSi<sub>2</sub> composites, including powder metallurgy, self-propagating high-temperature synthesis, spray processing, solid-state displacement reactions, and exothermic dispersion. Moreover, preliminary results aimed at improving the mechanical behaviour of MoSi<sub>2</sub> and MoSi<sub>2</sub> composites through selective, systematic, microstructural control are encouraging. A notable example of this approach is provided by the use of the XD<sup>TM</sup> technique, which allows for the selective precipitation of a large volume fraction of fine, well-dispersed particles. It is clear, however, that further improvements in the microstructure and behaviour of MoSi<sub>2</sub> are possible through the judicious combination of several synthesis techniques. For example, the introduction of solid-state reactions during plasma processing provides a unique opportunity to dramatically accelerate otherwise sluggish kinetic reactions, and thereby selectively form a distribution of desirable dispersoids in a one-step operation.

Examination of the oxidation behaviour and the mechanical properties of MoSi<sub>2</sub>-based composites reveals that SiC is by far the most oxidation-resistant reinforcement and yields the most encouraging mechanical property improvements. For example, the room temperature fracture toughness was significantly improved from  $\sim 2.5$  to  $\sim 9 \text{ MPa m}^{1/2}$  by the incorporation of SiC. At elevated temperatures, metallic reinforcements such as Nb, Ta and W, not only degrade the oxidation resistance of composites during exposure to an oxygen environment, but also react with MoSi<sub>2</sub> to form three-component intermetallics. Oxide reinforcements are also capable of providing a significant improvement on mechanical behaviour, especially ZrO<sub>2</sub>. However, enhanced oxygen diffusion at elevated temperatures weakens the oxidation resistance of oxide-reinforced MoSi<sub>2</sub> composites. Therefore utilization of oxides as reinforcements in MoSi<sub>2</sub> is conditional, depending on the operating temperatures.

Moreover, the addition of other reinforcements, such as  $TiB_2$ , C,  $Si_3N_4$ , may be capable of improving the mechanical properties of  $MoSi_2$ -based composites.

Regarding creep behaviour, it is extremely critical that the  $SiO_2$  phase be completely eliminated for improved creep resistance. A stress exponent in the vicinity of 3 was often reported for both monolithic and composite  $MoSi_2$ , suggesting that dislocation motion is responsible for the creep deformation. Furthermore, the observed high stress-exponent values can be attributed to a threshold stress phenomenon at the low stress condition and a change in rate-controlling mechanism from dislocation glide to dislocation climb as temperature increases.

On the basis of the above findings, it is evident that  $MoSi_2$  yields attractive combinations of elastic properties and oxidation resistance. These encouraging preliminary findings indicate that the utilization of  $MoSi_2$ -based composites as elevated-temperature structural materials is very promising. It is also evident however, that an understanding of the increasingly complex synthesis schemes will be necessary before  $MoSi_2$  composites are widely utilized as elevated-temperature engineering materials.

### Acknowledgment

The authors wish to express their gratitude to the Army Research Office (DAAL03-92-G-0181) for financial support and encouragement.

### References

- S. P. MURARKA, *J. Vacuum Sci. Technol.* **17** (1980) 775.
- B. K. BHATTACHARYYA, D. M. BYLANDER and L. KLEINMAN, *Phys. Rev. B* **31** (1985) 2049.
- B. K. BHATTACHARYYA, D. M. BYLANDER and L. KLEINMAN, *ibid.* **31** (1985) 5462.
- M. AZIZAN, R. BAPTIST, T. A. NGUYEN TAN and J. Y. VEUILLIN, *Appl. Surf. Sci.* **38** (1989) 117.
- A. CLIMENT, J. PERRIERE, A. LAURENT, B. LAVERNHE, R. PEREZ-CASERO and J. M. MARTINEZ-DUART, *ibid.* **38** (1989) 125.
- J. SCHLICHTING, *High Temp.-High Pressure* **10** (1978) 241.
- F. D. GAC and J. J. PETROVIC, *J. Amer. Ceram. Soc.* **68** (1985) C-200.
- A. K. VASUDEVAN and J. J. PETROVIC, *Mater. Sci. Engng* **A155** (1992) 1.
- T. C. LU, Y. G. DENG, C. G. LEVI and R. MEHRABIAN, in "Advanced Metal Matrix Composites for Elevated Temperatures Conference Proceedings", edited by M. N. Gungor, E. J. Lavernia and S. G. Fishman (ASM Internat. Materials Park, Ohio, 1991) p. 11.
- T. C. LU, A. G. EVANS, R. J. HECHT and R. MEHRABIAN, *Acta Metall. Mater.* **39** (1991) 1853.
- P. J. MESTCHER and D. S. SCHWARTZ, *JOM* **41** (1989) 52.
- J. D. COTTON, Y. S. KIM and M. J. KAUFMAN, *Mater. Sci. Engng* **A144** (1991) 287.
- M. J. MALONEY and R. J. HECHT, *ibid.* **A155** (1992) 19.
- Y. UMAKOSHI, T. HIRANO, T. SAKAGAMI and T. YAMANE, *Scripta Metall.* **23** (1989) 87.
- Y. UMAKOSHI, T. HIRANO, T. SAKAGAMI and T. YAMANE, *Acta Metall. Mater.* **38** (1990) 909.
- Y. UMAKOSHI, T. SAKAGAMI, T. YAMANE and T. HIRANO, *Phil. Mag. Lett.* **59** (1989) 159.
- O. UNAL, J. J. PETROVIC, D. H. CARTER and T. E. MITCHELL, *J. Amer. Ceram. Soc.* **73** (1990) 1752.
- M. NAKAMURA, S. MATSUMOTO and T. HIRANO, *J. Mater. Sci.* **25** (1990) 3309.
- T. HIRANO, M. NAKAMURA, K. KIMURA and Y. UMAKOSHI, *Ceram. Engng Sci. Proc.* **12** (1991) 1619.
- K. KIMURA, M. NAKAMURA and T. HIRANO, *J. Mater. Sci.* **25** (1990) 2487.
- R. R. GILER, *Metals Engineering Quarterly* Nov. (1973) 48.
- V. BIZZARI, B. LINDER and N. LINDSKOG, *Metals Mater.* **5** (1989) 403.
- V. BIZZARI, B. LINDER and N. LINDSKOG, *Ceram. Bull.* **68** (1989) 1834.
- P. S. KISLY and V. Y. KODASH, *Ceramics Intl* **15** (1989) 189.
- A. J. MOULSON and J. M. HERBET, in "Electroceramics: Materials, Properties, Application" (Chapman and Hall, New York, 1991) p. 121.
- J. J. LEWANDOWSKI, D. DIMIDUK, W. KERR and M. G. MENDIRATTA, in "High Temperature/High-Performance Composites", Materials Research Society Symposium Proceedings Vol. 120, edited by F. D. Lemkey, A. G. Evans, S. G. Fishman and J. R. Strife (Materials Research Society, Pittsburgh, Pennsylvania, 1988) p. 103.
- J. J. PETROVIC and R. E. HONNELL, *Ceram. Eng. Sci. Proc.* **11** (1990) 734.
- R. G. CASTRO, R. W. SMITH, A. D. ROLLETT and P. W. STANEK, *Scripta Metall. Mater.* **26** (1992) 207.
- R. G. CASTRO, R. W. SMITH, A. D. ROLLETT and P. W. STANET, *Mater. Sci. Engng* **A155** (1992) 101.
- D. H. CARTER and P. L. MARTIN, in "Intermetallic Matrix Composites", Materials Research Society Symposium Proceedings Vol. 194, edited by D. L. Anton, R. McMeeking, D. Miracle and P. Martin (Materials Research Society, Pittsburgh, Pennsylvania, 1990) p. 131.
- L. XIAO, Y. S. KIM and R. ABBASCHIAN, *ibid.* p. 399.
- S. MALOY, A. H. HEUER, J. LEWANDOWSKI and J. J. PETROVIC, *J. Amer. Ceram. Soc.* **74** (1991) 2704.
- T. C. CHOU, *Scripta Metall. Mater.* **24** (1990) 1131.
- W. S. GIBBS, J. J. PETROVIC and R. E. HONNELL, *Ceram. Engng Sci. Proc.* **8** (1987) 645.
- D. H. CARTER, J. J. PETROVIC, R. E. HONNELL and W. S. GIBBS, *ibid.* **10** (1989) 1121.
- D. H. CARTER and G. F. HURLEY, *J. Amer. Ceram. Soc.* **70** (1987) C-79.
- J.-M. YANG, W. KAI and S. M. JENG, *Scripta Metall.* **23** (1989) 1953.
- J. J. PETROVIC and R. E. HONNELL, *J. Mater. Sci. Lett.* **9** (1990) 1083.
- W. SCHMID, W. WRUSS, R. STROH, T. EKSTROM and B. LUX, *Ceramic Forum Intl* **67** (1990) 245.
- A. V. NOVIKOV, V. F. MELEKHIN and V. S. PEGOV, *Refractories* **30** (1990) 426.
- E. N. KULENKO and B. I. POPLYAK, *ibid.* **30** (1990) 418.
- J.-M. YANG and S. M. JENG, in "Intermetallic Matrix Composites", Materials Research Society Symposium Proceedings Vol. 194, edited by D. L. Anton, R. McMeeking, D. Miracle and P. Martin (Materials Research Society, Pittsburgh, Pennsylvania, 1990) p. 138.
- J. J. PETROVIC and R. E. HONNELL, *J. Mater. Sci.* **25** (1990) 4453.
- A. K. BATTACHARYA and J. J. PETROVIC, *J. Amer. Ceram. Soc.* **74** (1991) 2700.
- J. J. PETROVIC, R. E. HONNELL, T. E. MITCHELL, R. K. WADE and K. J. McCLELLAN, *Ceram. Engng. Sci. Proc.* **12** (1991) 1633.
- S. C. TUFFE, K. P. PLUCKNETT and D. S. WILKINSON, *ibid.* **14** (1993) 1199.
- K. SADANANDA, C. R. FENG, H. JONES and J. J. PETROVIC, *Mater. Sci. Engng* **A155** (1992) 227.
- K. SADANANDA, H. JONES, J. FENG, J. J. PETROVIC and A. K. VASUDEVAN, *Ceram. Engng Sci. Proc.* **12** (1991) 1671.
- J. J. PETROVIC and A. K. VASUDEVAN, in "Intermetallic Matrix Composites II", Materials Research Society Symposium Proceedings Vol. 273, edited by D. Miracle, J. Graves

- and D. Anton (Materials Research Society, Pittsburgh, Pennsylvania, 1992) p. 229.
50. K. SADANANDA, C. R. FENG, in "Processing and Fabrication of Advanced Materials for High Temperature Applications II", edited by V. A. Ravi and T. S. Srivatsan (Minerals, Metals & Materials Society, Warrendale, Pennsylvania, 1993) p. 331.
  51. K. K. RICHARDSON and D. W. FREITAG, *Ceram. Engng Sci. Proc.* **12** (1991) 1679.
  52. R. M. AIKIN, Jr., *ibid.* **12** (1991) 1643.
  53. A. K. BHATTACHARYA and J. J. PETROVIC, *J. Amer. Ceram. Soc.* **75** (1992) 23.
  54. A. R. COX and R. BROWN, *J. Less-Common Metals* **6** (1964) 51.
  55. J. B. BERKOWITZ-MATTUCK, M. ROSETTI and D. W. LEE, *Metall. Trans.* **1** (1970) 479.
  56. S. M. TUOMINEN and J. M. DAHL, *J. Less-Common Metals* **81** (1981) 249.
  57. M. P. BOROM, R. B. BOLOM and M. K. BRUN, *Adv. Ceram. Mater.* **3** (1988) 607.
  58. J. COOK, R. MAHAPATRA, E. W. LEE, A. KHAN and J. WALDMAN, *Ceram. Engng Sci. Proc.* **12** (1991) 1656.
  59. P. J. MESCHTER, *Scripta Metall. Mater.* **25** (1991) 521.
  60. P. J. MESCHTER, in "High Temperature Ordered Intermetallic Alloys", Materials Research Society Symposium Proceedings Vol. 213, edited by L. Johnson, D. P. Hope and J. O. Stiegler (Materials Research Society, Pittsburgh, Pennsylvania, 1991) p. 1027.
  61. T. C. CHOU and T. G. NIEH, *Scripta Metall. Mater.* **26** (1992) 1637.
  62. T. C. CHOU and T. G. NIEH, *ibid.* **27** (1992) 19.
  63. M. KOIZUMI and M. NISHIHARA, in "Isostatic Pressing Technology and Applications" (Elsevier, London, New York, 1991) p. 181.
  64. H. V. ATKINSON and B. A. RICKINSON, in "Hot Isostatic Processing" (Adam Hilger, Bristol, Philadelphia, New York, 1991) p. 9.
  65. H. A. KUHN, in "Powder Metallurgy Processing", edited by H. A. Kuhn and A. Lawley (Academic Press, New York, 1978) p. 99.
  66. D. L. JOHNSON, *Scripta Metall.* **3** (1969) 567.
  67. R. M. SPRIGGS and S. K. DUTTA, in "Sintering and Related Phenomena", edited by G. C. Kuczynski (Plenum, New York, London, 1973) p. 369.
  68. M. R. NOTIS, R. H. SMOAK and V. KRISHNAMACHARI, in "Sintering and Catalysis", edited by G. C. Kuczynski (Plenum, New York, London, 1975) p. 493.
  69. D. S. WILKINSON and M. F. ASHBY, *ibid.* p. 473.
  70. R. R. RICE, *Ceram. Engng Sci. Proc.* **11** (1990) 1226.
  71. R. RICE, in "Advanced Ceramic Processing and Technology", edited by J. G. P. Binner (Noyes Publication, Park Ridge, New Jersey, 1990) p. 173.
  72. N. CLAUSSEN and J. JAHN, *J. Amer. Ceram. Soc.* **63** (1980) 228.
  73. R. P. MESSNER and Y.-M. CHIANG, *Ceram. Engng Sci. Proc.* **9** (1988) 1052.
  74. Y.-M. CHIANG, J. S. HAGGERTY, R. P. MESSNER and C. DEMETRY, *Ceram. Bull.* **68** (1989) 420.
  75. R. P. MESSNER and Y.-M. CHIANG, *J. Amer. Ceram. Soc.* **73** (1990) 1193.
  76. M. M. WEISER, S. R. SMELSER and J. J. PETROVIC, in "Intermetallic Matrix Composites", Materials Research Society Symposium Proceedings Vol. 194, edited by D. L. Anton, R. McMeeking, D. Miracle and P. Martin (Materials Research Society, Pittsburgh, Pennsylvania, 1990) p. 53.
  77. J. KAJUCH and K. VEDULA, in "Advances in Powder Metallurgy", in Proceedings of the 1990 Powder Metallurgy Conference and Exhibition, Part 2, (Metal Powder Ind. Fed., Amer. Powder Met. Inst., Princeton, New Jersey, 1990) p. 187.
  78. R. K. VISWANADHAM, S. K. MANNAN and S. KUMAR, *Scripta Metall.* **22** (1988) 1011.
  79. M. ATZMON, in "Solid State Powder Processing", edited by A. H. Chauer and J. J. de Barbadillo (Minerals, Metals & Materials Society, Warrendale, Pennsylvania, 1990) p. 173.
  80. M. ATZMON, *Mater. Sci. Engng* **A134** (1991) 1326.
  81. M. ATZMON, *Metall. Trans.* **23A** (1992) 49.
  82. R. SUNDARESAN and F. H. FROES, *JOM* **39** (1987) 22.
  83. R. SUNDARESAN and F. H. FROES, *Metal Powder Report* **44** (1989) 195.
  84. S. OCHIAI, T. SHIROKURA, D. TAKASHI, K. YOSHIMARU and Y. KOJIMA, *ISIJ Intl* **31** (1991) 1106.
  85. F. H. FROES, C. SURYANARAYANA, E. J. LAVERNIA and G. E. BOBECK, *SAMPE Quarterly* July (1991) 11.
  86. D. PARLAPANSKI, S. DENEV, S. RUSEVA and E. GATEV, *J. Less-Common Metals* **171** (1991) 231.
  87. M. A. MORRIS and D. G. MORRIS, *Mater. Sci. Engng* **A110** (1989) 139.
  88. M. A. MORRIS and D. G. MORRIS, *ibid.* **A136** (1991) 59.
  89. S. G. YOUNG and G. R. ZELLARS, *Thin Solid Films* **53** (1978) 241.
  90. B. T. McDERMOTT and C. C. KOCH, *Scripta Metall.* **20** (1986) 669.
  91. R. L. WHITE and W. D. NIX, in "New Developments and Applications in Composites", edited by D. Kuhlmann-Wilsdorf and W. C. Harrigan (TMS, AIME, Warrendale, Pennsylvania, 1979) p. 78.
  92. A. U. SEYBOLT, *Trans. ASM.* **59** (1966) 860.
  93. M. YAMAZAKI, Y. KAWASAKI and K. KUSUNOKI, in "Structural Applications of Mechanical Alloying", edited by F. H. Froes and J. J. deBarbadillo (ASM International, Materials Park, Ohio, 1990) p. 33.
  94. M. A. DAEUBLER and D. FROSCHAMMER, *ibid.* p. 119.
  95. G. D. SMITH and P. GANESAN, *ibid.* p. 109.
  96. T. OHASHI and Y. TANAKA, *Mater. Trans. JIM* **32** (1991) 587.
  97. N. IWATOMO and S. UESAKA, in "Ceramic Powder Processing IV", Proceedings of the Fourth International Conference on Ceramic Powder Processing Science, edited by S.-I. Hirano, G. L. Messing and H. Hausner (American Ceramic Society, Westerville, Ohio, 1990) p. 177.
  98. E. MA, J. PAGAN, G. GRANFORD and M. ATZMON, *J. Mater. Res.* **8** (1993) 1836.
  99. S. JAYASHANKAR and M. J. KAUFMAN, *Scripta Metall. Mater.* **26** (1992) 1245.
  100. R. B. SCHWARZ, S. R. SRINIVASAN, J. J. PETROVIC and C. J. MAGGIORE, *Mater. Sci. Eng.* **A155** (1992) 75.
  101. A. A. ZENIN, A. G. MERZHANOV and G. A. NERSISYAN, *Combust. Explos. Shock Waves* (English Translation) **17** (1981) 63.
  102. T. BODDINGTON, P. G. LAYE, J. TIPPING and D. WHALLY, *Combust. Frame* **63** (1986) 359.
  103. Z. A. MUNIR, *Metall. Trans.* **23A** (1992) 7.
  104. A. R. SARKISYAN, S. K. DOLUKHANYAN, I. P. BOROVINSKAYA and A. G. MERZHANOV, *Combust. Explos. Shock Waves* (English Translation) **14** (1978) 310.
  105. T. S. AZATYAN, V. M. MALTSEV, A. G. MERZHANOV and V. A. SELEZNEV, *ibid.* **15** (1978) 35.
  106. J. TRAMBUKIS and Z. A. MUNIR, *J. Amer. Ceram. Soc.* **73** (1990) 1240.
  107. A. K. BHATTACHARYA, *ibid.* **74** (1991) 2707.
  108. S. C. DEEVI, *Mater. Sci. Engng* **A149** (1992) 241.
  109. A. K. BHATTACHARYA, *Ceram. Engng Sci. Proc.* **12** (1991) 1697.
  110. J. W. McCAULEY, *ibid.* **11** (1990) 1137.
  111. J. A. PUSZYNSKI, S. MAJOROWSKI and V. HLAVACEK, *ibid.* **11** (1990) 1182.
  112. R. W. RICE, *ibid.* **11** (1990) 1203.
  113. B. H. RABIN and R. N. WRIGHT, *Metall. Trans.* **A23** (1992) 35.
  114. I. SONG and N. H. THADHANI, *ibid.* **A23** (1992) 41.
  115. B. R. KRUEGER, A. H. MUTZ and T. VREELAND, Jr., *ibid.* **A23** (1992) 55.
  116. H. C. YI, J. J. MOORE and A. PETRIC, *ibid.* **A23** (1992) 59.
  117. J.-P. LEBRAT, A. VARMA and A. E. MILLER, *ibid.* **A23** (1992) 69.
  118. D. A. HOKE, M. A. MEYERS, L. W. MEYER and G. T. GARY III, *ibid.* **A23** (1992) 77.
  119. P. W. FUERSCHBACH and G. A. KNOROVSKY, *Welding J.* **70** (1991) S287.

120. R. W. SMITH, E. HARZENSKI and T. ROBISCH, in "Thermal Spray Research and Applications", edited by T. F. Bernecki (ASM International, Materials Park, Ohio, 1991) p. 617.
121. E. J. LAVERNIA, *Intl J. Rapid Solid.* **5** (1989) 47.
122. P. MATHUR and A. LAWLEY, *Acta Metall.* **37** (1989) 429.
123. A. R. E. SINGER, *Mater. Sci. Engng.* **135A** (1991) 13.
124. P. MATHUR and A. LAWLEY, *Mater. Sci. Engng* **142A** (1991) 261.
125. X. LIANG and E. J. LAVERNIA, *Acta Metall. Mater.* **40** (1992) 3003.
126. E. J. LAVERNIA, J. D. AYERS and T. S. SRIVATSAN, *Intl Mater. Rev.* **37** (1992) 1.
127. M. R. JACKSON, J. R. RAIRDEN, J. S. SMITH and R. W. SMITH, *JOM* **33** (1981) 23.
128. P. A. SIEMERS, M. R. JACKSON, R. L. MEHAN and J. R. RAIRDEN III, *Ceram. Engng Sci. Proc.* **6** (1985) 896.
129. P. FAUCHAIS, A. VARDELLE and M. VARDELLE, *Ceram. Intl.* **17** (1991) 367.
130. M. F. SMITH, D. T. MCGUFFIN, J. A. HENFLING and W. B. LENLING, in "Thermal Spraying Coating: Properties, Processes and Applications" edited by T. F. Bernecki (ASM International, Materials Park, Ohio, 1992) p. 27.
131. J. E. NERZ, B. A. KUSHNER, Jr. and A. J. ROTOLICO, *ibid.* p. 121.
132. R. TIWARI, H. HERMAN and S. SAMPATH, in "High Temperature Ordered Intermetallic Alloys", Materials Research Society Symposium Proceedings Vol. 213, edited by L. Johnson, D. P. Hope and J. O. Stiegler (Materials Research Society, Pittsburgh, Pennsylvania, 1991) p. 807.
133. Z. Z. MUTASIM and R. W. SMITH, "Thermal Plasma Applications in Materials and Metallurgical Processing", edited by N. El-Kaddah (Minerals, Metals & Materials Society, Warrendale, Pennsylvania, 1992) p. 269.
134. J. KARTHIKEYAN, R. RATNARAJ, A. J. HILL, Y. C. FAYMAN and C. C. BERNDT, in "Thermal Spraying Coating: Properties, Processes and Applications" edited by T. F. Bernecki (ASM International, Materials Park, Ohio, 1992) p. 497.
135. S. OKI, S. GOHDA, T. SHOMURA, T. H. KIMURA and T. YOSHIOKA, *ibid.* p. 491.
136. R. TIWARI, H. HERMAN and S. SAMPATH, *Mater. Sci. Engng* **A155** (1992) 95.
137. Y. L. JENG, J. WOLFENSTINE, E. J. LAVERNIA, D. E. BAILEY and A. SICKINGER, *Scripta. Metall. Mater.* **28** (1993) 453.
138. Y. L. JENG, E. J. LAVERNIA, J. WOLFENSTINE, D. E. BAILEY and A. SICKINGER, *Scripta. Metall. Mater.* **29** (1993) 107.
139. C. WAGNER, *Z. Anorg. Allg. Chem.* **236** (1938) 320.
140. C. WAGNER, *J. Electrochem. Soc.* **103** (1956) 571.
141. C. WAGNER, *Z. Phys. Chem.* **64** (1969) 49.
142. R. A. RAPP, A. EZIS and G. J. YUREK, *Metall. Trans.* **4** (1973) 1283.
143. G. J. YUREK, R. A. RAPP and J. P. HIRTH, *ibid.* **4** (1973) 1293.
144. S. R. SHATYNSKI, J. P. HIRTH and R. A. RAPP, *ibid.* **10A** (1979) 591.
145. G. J. YUREK, R. A. RAPP and J. P. HIRTH, *ibid.* **10A** (1979) 1473.
146. C. TANGCHITVITTAYA, J. P. HIRTH and R. A. RAPP, *ibid.* **13A** (1982) 585.
147. C. H. HENAGER, Jr., J. L. BRIMHALL and J. P. HIRTH, *Scripta. Metall. Mater.* **26** (1992) 585.
148. C. H. HENAGER, Jr., J. L. BRIMHALL and J. P. HIRTH, *Mater. Sci. Engng* **A155** (1992) 109.
149. J. M. BRUPBACHER, L. CHRISTODOVLOU and D. C. NAGLE, XD<sup>TM</sup>, U.S. Patent No. 4710348
150. A. R. C. WESTWOOD, *Metall. Trans.* **19A** (1988) 749.
151. L. CHRISTODOULOU, P. A. PARRISH and C. R. CROWE, in "High Temperature/High Performance Composites", Materials Research Society Symposium Proceedings Vol. 120, edited by F. D. Lemkey, S. G. Fishman, A. G. Evans and J. R. Strife (Materials Research Society, Pittsburgh, Pennsylvania, 1988) p. 29.
152. L. WANG and R. J. ARSENAULT, *Metall. Trans.* **22A** (1991) 3013.
153. D. D. VVEDENSKY, M. E. EBERHART, L. CHRISTODOULOU, S. CRAMPIN and J. M. MacLAREN, *Mater. Sci. Engng* **A126** (1990) 33.
154. D. E. LARSEN, L. CHRISTODOULOU, S. L. KAMPE and P. SADLER, *ibid.* **A144** (1991) 45.
155. E. W. LEE, J. COOK, A. KHAN, R. MAHAPATRA and J. WALDMAN, *JOM* **43** (1991) 54.
156. R. M. AIKIN, Jr., *Mater. Sci. Engng* **A155** (1992) 121.
157. D. A. BERZTISS, R. R. CERCHIARA, E. A. GULBRANSEN, F. S. PETTIT and G. H. MEIER, *ibid.* **A155** (1992) 165.
158. M. RUHLE and A. G. EVANS, *Prog. Mater. Sci.* **33** (1989) 85.
159. S. A. MALOY, J. J. LEWANDOWSKI, A. H. HEUER and J. J. PETROVIC, *Mater. Sci. Engng* **A155** (1992) 159.
160. E. M. LEVIN, in "Phase Diagram for Ceramists", edited by E. M. Levin, H. F. McMurdie, F. P. Hall, M. K. Reser and H. Inslay (American Ceramic Society, Columbus, Ohio, 1955-1959) p. 5.
161. W. A. KAYSSER and G. PETZOW, *Powder Metall.* **28** (1985) 145.
162. A. BASU and A. GHOSH, in "Advanced Metal Matrix Composites for Elevated Temperatures Conference Proceedings", edited by M. N. Gungor, E. J. Lavernia and S. G. Fishman (ASM Int. Materials Park, Ohio, 1991) p. 41.
163. S. BOSE, *Mater. Sci. Engng* **A155** (1992) 217.
164. S. M. WIEDERHORN, R. J. GETTINGS, D. E. ROBERTS, C. OSTERTAG and J. J. PETROVIC, *ibid.* **A155** (1992) 209.
165. M. SUZUKI, S. R. NUTT and R. M. AIKIN, Jr., in "Intermetallic Matrix Composites II", Materials Research Society Symposium Proceedings Vol. 273, edited by D. Miracle, J. Graves and D. Anton (Materials Research Society, Pittsburgh, Pennsylvania, 1992) p. 267.
166. M. SUZUKI, S. R. NUTT and R. M. AIKIN, Jr., *Mater. Sci. Engng* **A162** (1993) 73.

Received 12 January  
and accepted 30 September 1993